Journal of Human Genetics
https://doi.org/10.1038/s10038-020-0765-3

ARTICLE

A novel *ITPA* variant causes epileptic encephalopathy with multiple-organ dysfunction

Masamune Sakamoto[1,2] · Den Kouhei[1] · Muzhirah Haniffa[3] · Sebastián Silva[4] · Mónica Troncoso[5] · Paola Santander[5] · Valeria Schonstedt[6] · Ximena Stecher[6,7] · Nobuhiko Okamoto[8] · Kohei Hamanaka[1] · Takeshi Mizuguchi[1] · Satomi Mitsuhashi[1] · Noriko Miyake[1] · Naomichi Matsumoto[1]

Received: 17 January 2020 / Revised: 18 March 2020 / Accepted: 13 April 2020

Abstract

Inborn errors of metabolism can cause epileptic encephalopathies. Biallelic loss-of-function variants in the *ITPA* gene, encoding inosine triphosphate pyrophosphatase (ITPase), have been reported in epileptic encephalopathies with lack of myelination of the posterior limb of the internal capsule, brainstem tracts, and tracts to the primary visual and motor cortices (MIM:616647). ITPase plays an important role in purine metabolism. In this study, we identified two novel homozygous *ITPA* variants, c.264-1 G > A and c.489-1 G > A, in two unrelated consanguineous families. The probands had epilepsy, microcephaly with characteristic magnetic resonance imaging findings (T2 hyperintensity signals in the pyramidal tracts of the internal capsule, delayed myelination, and thin corpus callosum), hypotonia, and developmental delay; both died in early infancy. Our report expands the knowledge of clinical consequences of biallelic *ITPA* variants.

Introduction

Inosine triphosphate pyrophosphatase (ITPase), encoded by *ITPA* (MIM:147520, NM_033453.3), plays an important role in purine metabolism by catalyzing the phosphohydrolysis of inosine triphosphate (ITP) to inosine monophosphate (IMP). ITPase functions as a homodimeric protein; each monomer consists of 194 amino acids in eight exons [1]. ITPase has a central mixed β-sheet area that forms a platform to support two globular lobes; its substrate, ITP, binds in the lobes [2]. ITPase is localized in the cytoplasm and is constitutively expressed in various human tissues (https://www.genecards.org/cgi-bin/carddisp.pl?gene=ITPA).

In purine metabolism, two different pathways are recognized: de novo purine synthesis and purine salvage synthesis (Fig. 1). In these pathways, IMP, adenosine monophosphate (AMP), guanosine monophosphate (GMP), and xanthosine monophosphate (XMP) are synthesized. The noncanonical nucleotides (deoxy)ITP [(d)ITP] and (deoxy)xanthosine triphosphate [(d)XTP] are produced by deamination of (d)ATP and (d)GTP, respectively, or by phosphorylation of IMP and xanthosine monophosphate (XMP), respectively. ITPase plays an important role in conversion of (d)ITP/(d)XTP to IMP/XMP, preventing accumulation of (d)ITP/(d)XTP. The structural similarities

Supplementary information The online version of this article (https://doi.org/10.1038/s10038-020-0765-3) contains supplementary material, which is available to authorized users.

✉ Noriko Miyake
nmiyake@yokohama-cu.ac.jp

✉ Naomichi Matsumoto
naomat@yokohama-cu.ac.jp

1 Department of Human Genetics, Graduate School of Medicine, Yokohama City University, Yokohama, Japan

2 Department of Pediatrics, Graduate School of Medicine, Yokohama City University, Yokohama, Japan

3 Department of Genetics, Hospital Kuala Lumpur, Jalan Pahang, Malaysia

4 Child Neurology Service, Hospital de Puerto Montt, Puerto Montt, Chile

5 Child Neurology Service, Hospital San Borja Arriarán, Universidad de Chile, Santiago, Chile

6 Department of Radiology, Clínica Alemana de Santiago, Santiago, Chile

7 Department of Radiology, Facultad de Medicina Clínica Alemana, Universidad del Desarrollo, Santiago, Chile

8 Osaka Women's and Children's Hospital, Osaka, Japan

Published online: 14 May 2020

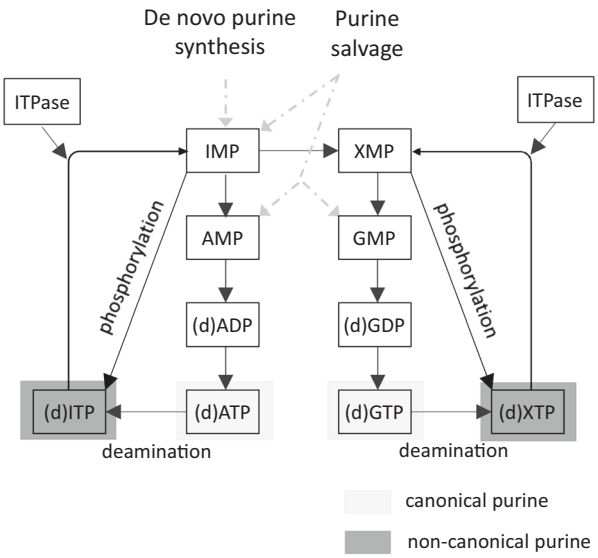

Fig. 1 Purine metabolism. IMP is synthesized either by the de novo purine synthesis route or the purine salvage route. (d)ITP is produced via phosphorylation of IMP or deamination of (d)ATP. ITPase plays an important role in conversion of (d)ITP/(d)XTP to IMP/XMP, preventing accumulation of ITP/XTP. (d)ATP/(d)GTP are canonical purines (shaded in light gray) and (d)ITP/(d)XTP are noncanonical purines (shaded in dark gray). IMP inosine monophosphate, (d)ITP deoxy inosine triphosphate, ATP adenosine triphosphate, ITPase inosine triphosphate pyrophosphatase, GTP guanosine triphosphate, XTP xanthosine triphosphate, XMP xanthosine monophosphate

between adenine, guanine, and hypoxanthine (the nucleobase of ITP) make it plausible that ITP can act as an improper substrate and replace the canonical nucleotides AMP and GMP. Accumulation of (d)ITP leads to incorporation of inosine bases into DNA and RNA of yeast and E. coli [3], probably resulting in production of damaged DNA and nonfunctional RNAs. Analysis of the nucleotide content of total heart RNA of ITPase knockout mice revealed a high level of IMP, whereas IMP was undetectable in wild-type mice [4].

Itpa null mice show motor dysfunction, growth retardation, abnormal breathing, and cardiomyopathy but no epilepsy [4]. In humans, biallelic *ITPA* variants have been reported to cause epileptic encephalopathies with multiorgan dysfunction (MIM:616647) [5]. To our knowledge, six pathogenic variants have been reported [5–7]. All patients with biallelic *ITPA* variants show epilepsy, progressive microcephaly, hypotonia, and developmental delay. In addition, T2 hyperintensity of the pyramidal tracts in the internal capsule, delayed myelination, and thin corpus callosum on brain magnetic resonance imaging (MRI) are commonly observed in affected individuals. Some patients have cataracts or cardiomyopathy.

Here, we report two novel homozygous *ITPA* pathogenic variants in two unrelated affected individuals and describe their detailed clinical features.

Materials and methods

Sample and clinical information collection

Blood samples were collected from the patients and their parents after written informed consent was obtained. Detailed clinical information was obtained by the clinicians examining the patients. This study was approved by the Institutional Review Board of Yokohama City University of Medicine.

Whole-exome sequencing

Whole-exome sequencing (WES) was performed on each proband as previously described [8]. In brief, genomic DNA was isolated from peripheral blood leukocytes using QuickGene 610 L nucleic acid isolation system (Wako, Osaka, Japan). After shearing the DNA, genome partitioning was performed using the SureSelect XT Human All Exon v6 kit (Agilent Technologies, Santa Clara, CA, USA), and whole exome was sequenced on an Illumina NovaSeq sequencer (Illumina, San Diego, CA, USA) with 151-bp paired-end reads. Sequence reads were aligned to the human reference genome (UCSC hg19, NCBI build 37.1) and PCR duplicates were excluded using Novoalign v3.02 (http://www.novocraft.com/) and Picard v1.98 (http://picard.sourceforge.net/), respectively. Variant calling and annotation were performed using GATK UnifiedGenotyper (https://gatk.broadinstitute.org/) and ANNOVAR (http://annovar.openbioinformatics.org/). Common single-nucleotide polymorphisms with minor allele frequencies ≥1% in dbSNP 137 (https://www.ncbi.nlm.nih.gov/snp/) and variants that were observed in >5 of our 575 in-house Japanese control exomes were excluded from the candidate variants. Among the remaining rare variants, we focused on amino acid-altering or splice-affecting variants (±20 bp). Particular attention was paid to variants in known causative genes associated with epileptic encephalopathies. The candidate variants were validated by Sanger sequencing with an ABI Prism 3500 × 1 autosequencer (Life Technologies, Carlsbad, CA, USA), using genomic DNA of the patients and their parents as a PCR template.

Results

Clinical features

Patient 1 was the only child of healthy consanguineous parents; the parents are second cousins (Fig. 2a, family 1). There was no familial and perinatal history that could lead to the observed neurological problems in the proband. She was born at 37 gestational weeks with a birth weight of

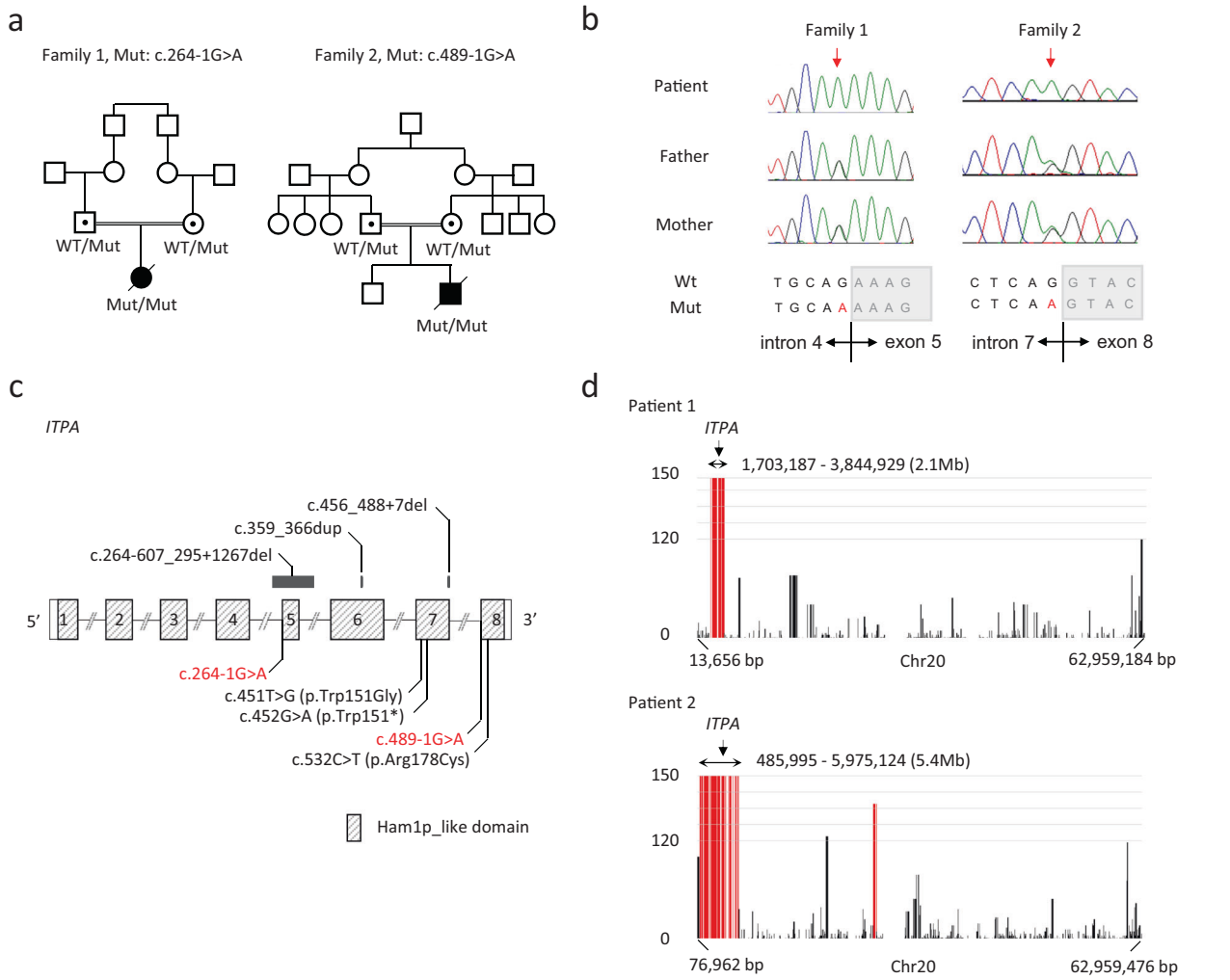

Fig. 2 **a** Pedigrees of unrelated families 1 and 2. In both families, consanguineous parents had the heterozygous variant (wild-type/mutant; WT/Mut) and patients had the homozygous variant. **b** Electropherograms of homozygous *ITPA* variants in patients 1 and 2. Both variants are located in canonical splice sites; locations of variants are shown by the red arrows. **c** Schematic presentation of pathogenic variants in *ITPA*. The variants found in this study are shown in red, numbered boxes indicate exons, and the Ham1p_like domain is shown as striped boxes spanning the eight exons. **d** Homozygous stretches in chromosome 20 in our two patients are shown with HomozygosityMapper (http://www.homozygositymapper.org/) using whole-exome sequencing data. Red indicates regions having more than 120 homozygous single nucleotide variants

2700 g (+0.2 SD), occipitofrontal circumference (OFC) of 33.5 cm (+0.6 SD), and length of 46 cm (−0.5 SD). She initially came to the hospital 1 day after receiving her fourth-month vaccination. She lost her contact and gaze and showed head deviation for 5 min with high fever. One week later, she was admitted to the hospital because of repeated similar episodes without fever and mild hypotonia. However, electroencephalogram (EEG), brain computed tomography, blood, and cerebrospinal fluid were normal. Brain MRI at the age of 5 months showed T2 hyperintensity of the pyramidal tracts in the internal capsule (Fig. 3a–e). From that point onward, the patient showed global developmental delay, progressive microcephaly, and intractable epilepsy. At 5 months, the EEG showed frequent inter-ictal epileptic activity in the parieto-occipital bilateral areas. The patient had low-set ears, a low nasal bridge, a long philtrum, epicanthal folds, and a short nose (Fig. 3k, l). After multiple admissions, the patient showed choreoathetosis-like movements accompanied by apnea. She died at 14 months following seizures and apnea.

Patient 2 was the second child of healthy and consanguineous parents (Fig. 2a, family 2); the parents are first-degree cousins. The proband's older brother was unaffected, and there was no family or perinatal history. The proband was born at 39 gestational weeks with a birth weight of 2900 g (−0.6 SD), OFC of 32 cm (−1.2 SD), and length of 50 cm (+0.6 SD). He was referred to the hospital at 3 months for increasing episodes of seizures. He showed microcephaly (OFC 36 cm, −2.4 SD), small anterior fontanelle, marked head lag with hypotonia, brisk reflexes, and

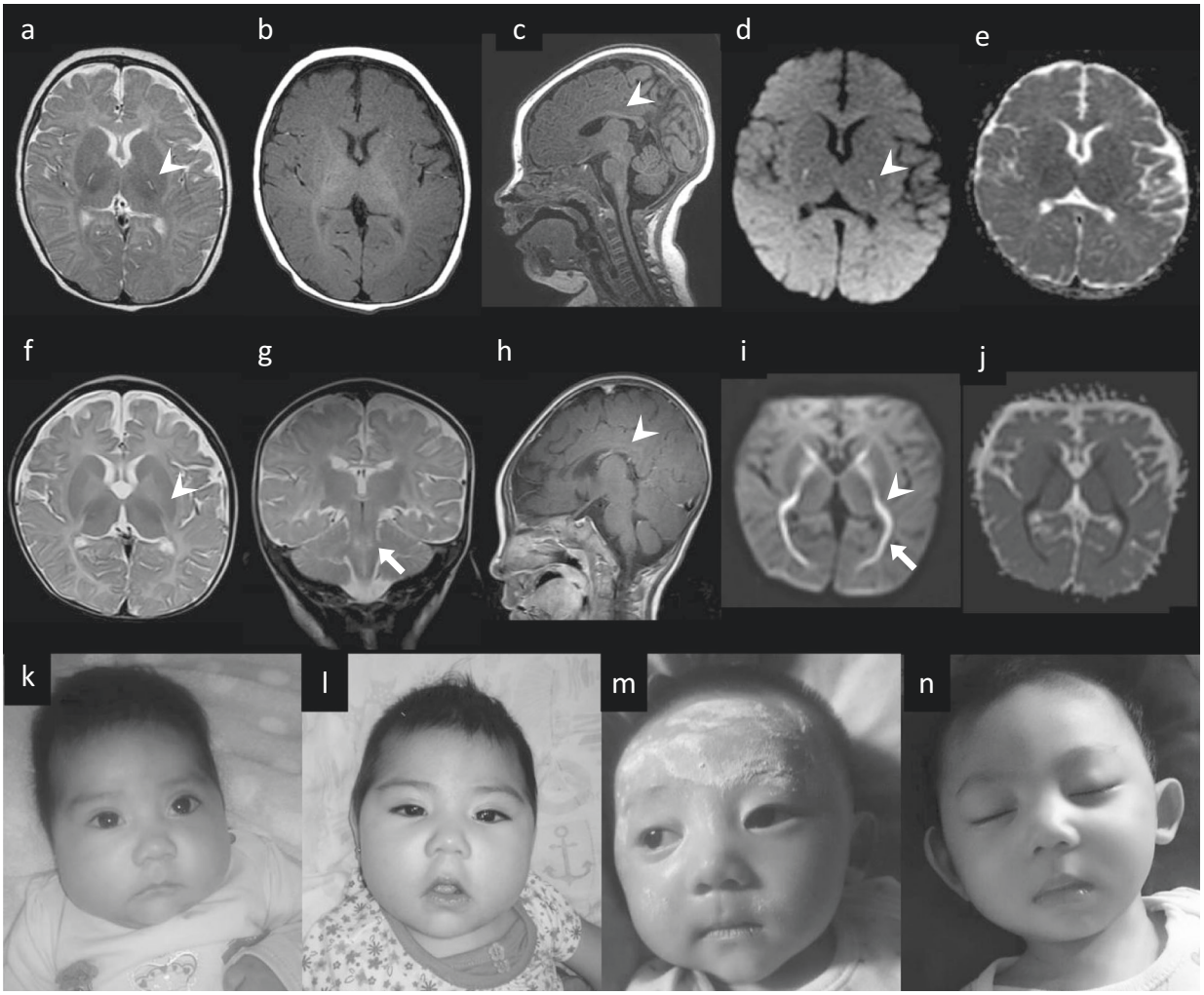

Fig. 3 Brain MRI and facial photographs of patients. Brain MRI in patient 1 (**a**–**e**) and patient 2 (**f**–**j**) at the age of 5 months. T2-weighted images (**a**, **f**, **g**); T1-weighted images (**b**, **c**, **h**); diffusion-weighted images (DWI) (**d**, **i**); ADC images (**e**, **j**) were shown. T2-weighted images and DWI in both patients show hyperintensity of pyramidal tracts in the internal capsule, delayed myelination, and thin corpus callosum (white arrowhead), corresponding to low signal on the ADC images (**e**, **j**). Patient 2 also showed T2 hyperintensity of the midbrain and increased DWI signal in optic radiation (**g**, **i**) (white arrow). Facial photographs of patient 1 (**k**, **l**) and patient 2 (**m**, **n**). Patient 1 at the age of 10 months (**k**) and at 1 year 2 months (**l**). Patient 2 at the age of 3 weeks (**m**) and at 4 months (**n**). Both patients had low-set ears, a low nasal bridge, a long philtrum, epicanthal folds, and a short nose

bilateral eye cataract. He had low-set ears, a low nasal bridge, a long philtrum, epicanthal folds, and a short nose (Fig. 3m, n). At the age of 5 months, he developed myoclonic jerks three to four times a day, and clonazepam was started. At 7 months, the patient showed global developmental delay, with no focusing, vocalizing, or smiling. At 10 months, seizures became intractable and an EEG showed polymorphic delta activity with occasional runs of spike-slow waves over the right posterior quadrant. Brain MRI at 5 months showed T2 hyperintensity of the pyramidal tracts in the internal capsule and mid brain, delayed myelination of the posterior limb of the internal capsule and optic radiation for visual field, cerebral atrophy, and thin corpus callosum (Fig. 3f–j). The patient died from pneumonia at 11 months of age.

Genetic analysis

WES was performed on the two probands. In patient 1, the mean read depth of the protein-coding regions was 59.4×, and an average of 91.1% of coding sequences (CDS) were sequenced by 20 or more reads. In patient 2, the mean read depth was 85.1× and an average of 97% of CDS were sequenced by 20 or more reads. We narrowed down the candidate variants based on autosomal dominant, autosomal recessive, and X-linked dominant and recessive models. We found pathogenic variants in *ITPA* that are known to cause autosomal recessive early infantile epileptic encephalopathy, 35 (MIM:616647), which matched our patients clinically.

WES revealed one homozygous *ITPA* variant in each patient: c.264-1 G > A in patient 1 and c.489-1 G > A in

Table 1 Clinical summary of patients having homozygous ITPA variants

	Our study		Kevelam et al. [5]							Kaur et al. [6]	Handley et al. [7]		Summary
Cases	Patient 1	Patient 2	1/I	2/I	3/I	4/II	7/II	5/ III	6/IV	Iv.2	VI:3	III:3	Total: 12 cases
ITPA variant	c.264-1G>A	c.489-1G>A	Del of 1.9 kbp*	Del of 1.9 kbp	Del of 1.9 kbp	c.452G>A	c.452G>A	c.532C>T	c.359_366dup	c.451T>G	c.452G>A	c.456_488+7del	Total: 8 variant types
Change	Splice site	Splice site	NMD	NMD	NMD	Nonsense	Nonsense	Missense	Frameshift	Missense	Nonsense	NMD	Disruptive: 6/8 (75%) missense: 2/8 (25%)
Zygosity	Homozygous	Homozygous	Homozygous	Homozygous	Homozygous	Homozygous	Homozygous	Homozygous	Homozygous	Homozygous	Homozygous	Homozygous	Homozygous: 12/12 (100%)
Sex	Female	Male	Male	Male	Male	Female	Male	Male	Female	Female	Male	Female	Male: 7/12 (58.3%)
Ethnic group	Chile	Malaysia	Morocco	Morocco	Morocco	Pakistan	Pakistan	Canada	Italy	N/A	Pakistan	Pakistan	
Consanguinity	+	+	+	+	+	+	+	−	N/A	+	+	+	10/11 (90.9%)
Birth data													
Birth weight (SD)	2.7 kg (0.2)	2.9 kg (−0.6)	3.3 kg (−0.5)	2.4 kg (<−2)	2.9 kg (−0.8)	3.3 kg (<−0.5)	2.2 kg (−0.5)	2.3 kg (−1.5)	2.4 kg (−1.8)	2.8 kg (−1.8)	N/A	2.8 kg	<−2 to 0.2 SD
OFC (SD)	33.5 cm (0.6)	32 cm (−1.2)	N/A	33 cm (−2)	33.8 cm (−1.5)	34 cm (−1)	33 cm (−1.5)	N/A	33 cm (−1.5)	32 cm (−2)	N/A	N/A	< −2 to 0.6 SD
Head growth													
Age at exzamination	14 months	10 months	8 months	28 months	30 months	5 months	3 months	26 months	25 months	9 months	N/A	N/A	3 to 30 months
OFC (SD)	40.5 cm (−3.6)	36.5 cm (−5.8)	40.5 cm (−3.5)	43.5 cm (−4)	40.5 cm (−5.5)	36.5 cm (−4)	34.8 cm (−3.5)	43.8 cm (−3.5)	39 cm (−6)	36.5 cm (−6.1)	N/A	42 cm (−7.6)	−6.1 to −3.5 SD
Microcephaly	+	+	+	+	+	+	+	+	+	+	+	+	12/12 (100%)
Clinical features													
Cataract	−	Cataract	Cataract	Cataract	Cataract	Normal	N/A	−	Normal	Cataract	Cataract	Cataract	7/11 (63.6%)
Developmental delay	Severe	+	Severe	Severe	Severe	Severe	Severe	Severe	Severe	+	+	Severe	12/12 (100%)
Hypotonia	+	+	+	+	+	+	+	+	+	+	+	+	12/12 (100%)
Epilepsy	+	+	+	+	+	+	+	+	+	+	+	+	12/12 (100%)
Cardiomyopathy	−	−	N/A	Dilated cardiomyopathy	−	Normal	−	Normal	Normal	Dilated cardiomyopathy	Mild dilation of left ventricle	Dilated cardiomyopathy	Cardiomyopathy: 3/11 (27.2%)
MRI findings													
Cerebral atrophy	−	+	−	−	−	−	N/A	−	−	+	N/A	N/A	2/9 (16.6%)
Delayed myelination	+	+	+	+	+	+	N/A	+	+	+	N/A	N/A	9/9 (100%)
Thin corpus callosum	+	+	+	+	+	+	N/A	+	+	+	N/A	N/A	9/9 (100%)
T2 hyper intensities in internal capsle	+	+	+	+	+	+	N/A	+	+	+	N/A	N/A	9/9 (100%)
Outcome	Death at 14 months	Death at 11 months	Death at 10 months	Death at 2 years	Death at 2 years	Death at 6 months	Death at 10 months	Death at 2 years	Alive	Death at 13 months	Death at 2 years	Death at 4 years	Death at <2 years 6/12 (50%) <5 years 11/12 (91.6%)
Cause of death	Sizures, apnea	Respiratory, infection	N/A	Cardiac failure	Respiratory, infection	Respiratory, infection	Seizures, infection	Seizures, infection		Seizures	N/A	Cardiac failure	

*c.264-607_295+1267del

N/A not available, *NMD* nonsense-mediated decay, *OFC* occipitofrontal circumference, *SD* standard deviation

patient 2. Autosomal recessive segregation of these variants was confirmed by Sanger sequencing (Fig. 2b). Both variants were absent from the Human Genetic Variation Database (HGVD; http://www.hgvd.genome.med.kyoto-u.ac.jp/) and our in-house controls. In gnomAD (https://gnomad.broadinstitute.org/), c.264-1 G > A is registered as extremely rare (minor allele frequency 0.05%) but only in the heterozygous state (not homozygous). The c.489-1 G > A variant is unregistered in gnomAD (Supplemental Table S1).

Using three different web-based prediction tools for splicing sites, we predicted the loss or weakness of original acceptor splice sites (Supplemental Fig. S1) and found no new potential acceptor sites within a 1-kb region of the variants.

HomozygosityMapper (http://www.homozygositymapper.org/) indicated that patient 1 had 3 homozygous stretch regions >2.0 Mb and patient 2 had 13 homozygous regions >2.0 Mb. *ITPA* variants were mapped to the third- and fourth-largest homozygous regions: Chr20:1,703,187–3,844,929 bp in patient 1 and Chr20:485,995–5,975,124 bp in patient 2 (Fig. 2d).

Discussion

To our knowledge, 11 *ITPA* variants have been reported, including 6 pathogenic variants (4 protein-truncating and 2 missense) [5–7]. We here describe two canonical splicing site variants. In Fig. 2c, all 8 pathogenic *ITPA* variants are shown. The functional domains of ITPA have been unknown, but all the mutations are within Ham1p-like domain which was predicted by SMART program (http://smart.embl-heidelberg.de/). The reported missense variants, c.451 T > G (p.Trp151Gly) and c.532 C > T (p.Arg178Cys), were predicted to be deleterious by various prediction programs; the Trp151 and Arg178 residues are each located in crucial substrate binding positions [5, 6]. The other 6 variants might lead to protein truncation. In gnomAD, 24 truncating variants are registered but all are heterozygous (Supplemental Table S1). These data support that biallelic loss-of-function variants of *ITPA* cause epileptic encephalopathy.

Table 1 shows the clinical features of 12 patients with *ITPA*-mutated epileptic encephalopathy. Interestingly, all patients have a homozygous variant, and 10 patients were born to parents with confirmed consanguinity. All patients showed epilepsy, progressive microcephaly, hypotonia, and developmental delay, together with characteristic brain MRI findings (T2 hyperintensity of the pyramidal tracts in the internal capsule, delayed myelination, and thin corpus callosum). Almost all patients died in early infancy (death at <2 years in 6 of 12 probands; death at <5 years in 11 of 12 probands). Seven patients had cataracts and three had cardiomyopathy (other one showed mild dilation of left ventricle). Most patients did not have perinatal problems but presented after birth with severe developmental delay, intractable epilepsy, postnatal progressive microcephaly, unique MRI findings, similar facial features (Fig. 3k–n) and, eventually, death in infancy or early childhood. Therefore, *ITPA*-mutated epileptic encephalopathy should be considered in patients with the clinical features described above.

Patient 2 had cataracts and microcephaly (Table 1), suggestive of Martsolf syndrome (MIM:212720). Martsolf syndrome is characterized by severely delayed development, postnatal microcephaly, congenital cataracts, and cardiomyopathy, and is associated with biallelic *RAB3GAP2* variants. Handley et al. analyzed 85 *RABGAP2*-negative patients with Martsolf or Martsolf-like syndrome, and identified two individuals with homozygous *ITPA* null variants [7]. It may be difficult to clinically differentiate *ITPA*-mutated and *RABGAP2*-mutated phenotypes. However, T2 hyperintensity of the pyramidal tracts in the internal capsule may be a clinical finding that is specific to *ITPA* variants, which could help differentiate the two diseases. In our cases, both patients had no *RAB3GAP2* variant.

The pathomechanism of the unique T2-high region in *ITPA*-mutated epileptic encephalopathy remains unclear. Kevelam et al. mentioned "Wallerian degeneration (WD)" as one possible explanation for it [5]. WD is a progressive anterograde disintegration of axons accompanying demyelination after an injury to the proximal axon or cell body [9]. In the process of WD, breakdown of myelin and resultant gliosis lead to increase hydrophilicity and hyperintensity on T2-weighed images [9]. We think this hypothesis is likely to explain the T2-high intensity.

In conclusion, we identified two novel splice-site variants in *ITPA* associated with epilepsy. Our report adds important information to our understanding of the clinical consequences of *ITPA* variants.

Acknowledgements We thank the affected individuals and their families for participating in this study. This work was supported by AMED under the grant numbers JP19ek0109280, JP19dm0107090, JP19ek0109301, JP19ek0109348, and JP18kk020501 (to NM); JSPS KAKENHI under the grant numbers JP17H01539 (to NM) and JP19H03621 (to NM); grants from the Ministry of Health, Labour, and Welfare (to NM); and the Takeda Science Foundation (to NM and NM). We thank Louise Adam, ELS(D), from Edanz Group (www.edanzediting.com/ac) for editing a draft of this manuscript.

Compliance with ethical standards

Conflict of interest The authors declare that they have no conflict of interest.

Publisher's note Springer Nature remains neutral with regard to jurisdictional claims in published maps and institutional affiliations.

References

1. Burgis NE. A disease spectrum for ITPA variation: advances in biochemical and clinical research. J Biomed Sci. 2016;23:73.
2. Stenmark P, Kursula P, Flodin S, Graslund S, Landry R, Nordlund P, et al. Crystal structure of human inosine triphosphatase. Substrate binding and implication of the inosine triphosphatase deficiency mutation P32T. J Biol Chem. 2007;282:3182–7.
3. Pang B, McFaline JL, Burgis NE, Dong M, Taghizadeh K, Sullivan MR, et al. Defects in purine nucleotide metabolism lead to substantial incorporation of xanthine and hypoxanthine into DNA and RNA. Proc Natl Acad Sci USA. 2012;109:2319–24.
4. Behmanesh M, Sakumi K, Abolhassani N, Toyokuni S, Oka S, Ohnishi YN, et al. ITPase-deficient mice show growth retardation and die before weaning. Cell Death Differ. 2009;16:1315–22.
5. Kevelam SH, Bierau J, Salvarinova R, Agrawal S, Honzik T, Visser D, et al. Recessive ITPA mutations cause an early infantile encephalopathy. Ann Neurol. 2015;78:649–58.
6. Kaur P, Neethukrishna K, Kumble A, Girisha KM, Shukla A. Identification of a novel homozygous variant confirms ITPA as a developmental and epileptic encephalopathy gene. Am J Med Genet A. 2019;179:857–61.
7. Handley MT, Reddy K, Wills J, Rosser E, Kamath A, Halachev M, et al. ITPase deficiency causes a Martsolf-like syndrome with a lethal infantile dilated cardiomyopathy. PLoS Genet. 2019;15:e1007605.
8. Miyake N, Fukai R, Ohba C, Chihara T, Miura M, Shimizu H, et al. Biallelic TBCD Mutations cause early-onset neurodegenerative encephalopathy. Am J Hum Genet. 2016;99:950–61.
9. Chen YJ, Nabavizadeh SA, Vossough A, Kumar S, Loevner LA, Mohan S. Wallerian degeneration beyond the corticospinal tracts: conventional and advanced MRI findings. J Neuroimaging. 2017;27:272–80.